Journal of Information Systems Engineering and Management
2025, 10(36s)
e-ISSN: 2468-4376
https://www.jisem-journal.com/

Research Article

Differential Function Fitting Neural Based Neural Network Energy Management Scheme for Plug-In Hybrid Electrical Vehicles with Real-Time Speed Profile and Optimal Battery Depth of Discharge

Muhamad Nabil Bin Hidayat[1], Naeem Hannoon*[2], Anshuman Satapathy[3], Dalina Binti Johari[4], Nor Farahaida Abdul Rahim[5]

[1,2,4,5]*School of Electrical Engineering, College of Engineering, Universiti Teknologi Mara, Shah Alam, Malaysia.*
[3]*Department of EEE, ITER, SOA Deemed to be University, Odisha, India*

ARTICLE INFO

Received: 30 Dec 2024

Revised: 19 Feb 2025

Accepted: 27 Feb 2025

ABSTRACT

This paper proposes the Differential Function Fitting Neural Based Neural Network Energy Management Scheme (DEMS) for PHEVs aimed at controlling the battery state of charge (SOC) and depth of discharge (DoD) based on the integration of the Pontryagin's Maximum Principle (PMP) and Artificial Neural Network (ANN). Recognizing the market development in the area of energy efficiency in PHEVs, the increase in battery performance is crucial. The proposed DEMS utilizes PMP for accurate energy management, and optimized learning from ANN for making dynamic changes as per dynamic driving environment. The system is also verified through MATLAB/Simulink models employing a rule-based dynamic programming (DP) strategy. Results demonstrate the proposed scheme's ability to maintain optimal SOC levels, reduce battery degradation, and improve overall vehicle efficiency. The DEMS significantly enhances battery performance, stability, and adaptability, offering a reliable solution for efficient PHEV operation under diverse driving scenarios. This approach contributes to the sustainable development of hybrid vehicle technologies by optimizing energy use and extending battery life.

Keywords: Plug-in Hybrid Electrical Vehicle (PHEV); State of Charge (SOC); Depth of Discharge (DoD); Ponytryagin's Maximum Principle (PMP); Artificial Neural Network (ANN); Differential Function Fitting Neural; Depth of Discharge (DoD)

INTRODUCTION

Energy conservation remains the key issue for the hybrid electric vehicles (HEVs) today [1]. Among HEVs, special interest has been oriented towards plug-in hybrid electric vehicles (PHEVs) since they can be charged via electricity grid and use conventional fuel [2], thus gaining more flexibility and lower emissions. The PHEVs, therefore, have enhanced battery capacity together with the power that is recharged from other supplementary sources in a manner that allows for a longer electric-only travel distance as compared to the basic hybrids [2]. Nevertheless, the health of batteries in PHEVs is still an issue due to many shortcomings in the existing battery management systems [3]. Reduced discharge efficiency, coupled with a lack of proper optimization techniques, enables the depth of discharge (DoD) to worsen the battery's capacity and energy losses [4]. The primary challenge in managing battery health is the absence of advanced battery management systems capable of real-time monitoring and adaptive control. Traditional systems rely on fixed thresholds and rule-based strategies, which are often inadequate for dynamic driving conditions. This results in suboptimal energy utilization and increased degradation rates.

Therefore, energy management schemes (EMS) are very important in the regulation of energy power in PHEV between the internal combustion engine, electric motor and battery system. As discussed, a good EMS helps with useful and efficient utilization of energy for increasing the life of batteries as well as the fuel efficiency [5]. Several approaches towards the implementation of the energy management system in PHEVs included the rule based, the optimization based, and the machine learning based has been discussed in the literature for EMS in PHEVs. The rule-based approach is more straightforward to develop, requiring less computational resources and provides energy allocation to fulfill a particular system with the help of a set of pre-established rules [6]. But they fail to

Journal of Information Systems Engineering and Management
2025, 10(36s)
e-ISSN: 2468-4376
https://www.jisem-journal.com/

Research Article

deliver in terms of dynamic changes in engine efficiency lacks adaptability to driving situations [6]. This can lead to less-than-optimal fuel efficiency and energy management of any type of equipment.

The optimization based, and the machine learning based has been discussed in the literature for EMS in PHEVs. Despite their complexity, optimization-based approaches for driving systems have number of drawbacks. These methods may necessitate massive computation which makes them incapable of real-time applications [7]. Besides, most of them are typically optimized for certain driving conditions and can perform poorly in dynamic driving situations [8]. In addition, these strategies may fail to respond to changes in driving behavior within a short period of time and thus affect total levels of productivity [9]. Finally, these models are highly complex, leading to oversimplification of real-life driving systems [7] whereby certain interactions may not be captured and therefore the result are sub-optimal solutions. In contrast, machine learning-based approaches harness data-driven models to predict optimal energy distribution [10]. This adaptability enhances efficiency by allowing systems to learn from previous data and adjust in real-time to changing conditions. Such methods can better accommodate the variability inherent in driving scenarios, leading to improved performance [10].

Lastly, this paper investigates how to extend optimization-based techniques, including Pontryagin's Minimum Principle (PMP), with machine learning-based techniques, including Artificial Neural Networks (ANN). propose a system that would make use of optimization techniques to achieve the most optimal solution in energy management with the help of machine learning capability to make it more adaptive and effective. This integration is anticipated to enhance the fuel economy and battery durability primarily under real-world driving conditions.

MODELLING AND POWERTRAIN OF PHEV

Plug-In Hybird Electrical Vehicle (PHEV)

Figure. 1 shows the components of PHEV that will be used as the main model of this study. The battery gains its supplies from the EGU which consists of an integrated-starter-generator (ISG) and diesel engine [8]. This car weighs about 9 tons and a length of about 3.84 meters. The vehicle's specification is 133 kw (99 KW). The car can travel for 300 kilometers on a single charge. Level 2 charging takes 6.5 hours, while Level 3 fast charging only takes 35 minutes for a full charge. Figure. 1 shows the part of the PHEV model.

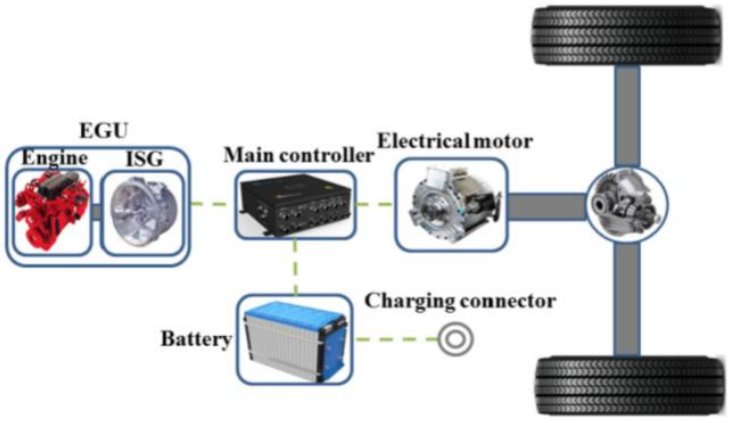

Figure. 1: Plug-In Hybrid Electrical Vehicle Powertrain [11].

In this vehicle, fuel for the EGU and battery that can be recharged by external sources as this is an improved version of hybrid electric vehicles (HEV) [12]. When the battery is fully charged, PHEV operates as EV in all electrical range (AER) of 30-60km [13] and then switches to hybrid mode when battery reaches its predefined soc or vehicle [12]. Below is the power balance equation of PHEV model.

Journal of Information Systems Engineering and Management
2025, 10(36s)
e-ISSN: 2468-4376
https://www.jisem-journal.com/

Research Article

$$P_V = \frac{1}{3600}\left(mgfV + \frac{C_d A}{21.15}V^3 + \xi m\frac{dv}{dt}V\right) \quad (1)$$

V represents the speed, ξ is the equivalent mass inertia and the rest specifications of this powertrain are summarized in Table. 1.

Table 1. Vehicle physical parameter

Parameters	Values
The gross mass, m	3628 kg
The rolling resistance coefficient, f	0.015
Air density, ρ	1.225 kg/m^3
Frontal area, A	0.5 m^2
The air drag coefficient, C_d	0.9
Gravity, g	9.81 m^2/s
Wheel diameter	0.406 m
Drive train efficiency	0.8

Table 2. Outline specifications for the operational limits of a vehicle's motor, covering both torque and speed ranges.

Table 2. Vehicle motor limitation

Motor Limitation	Values
Torque maximum limit, T_{max}	26 Nm
Torque lower limit T_{min}	0.1 Nm
Maximum speed, V_{max}	8200 rpm
Minimum speed, V_{min}	1 rpm

Battery Model

In this paper, a single lithium-ion phosphate battery with a 45Ah capacity and 450V nominal voltage is used. Battery dynamics, specifically open-circuit voltage and internal resistance are modeled as functions of the SOC using the internal resistance method Eq.2

$$P_{battery} = P_B + P_L = P_B + I_B{}^2 R_B \quad (2)$$

Where $P_{battery}$ represents the battery's internal rated power, P_B is its terminal battery power, P_L is the load power; I_B represents as the total battery current, and battery is the equivalent internal resistance represents the R_B. The battery equivalent circuit is illustrated in **Error! Reference source not found.**.

Figure 2. Battery Equivalent Circuit

Journal of Information Systems Engineering and Management
2025, 10(36s)
e-ISSN: 2468-4376
https://www.jisem-journal.com/

Research Article

The rate at which the battery's capacity decreases during the charge-discharge cycle is contingent upon both temperature and current. The point at which a battery's capacity drops to 80% of its declared capacity [14] is known as the battery's end of lifespan (EOF) [15]. In this case the battery life decline is computed using the empirical model which is described in Eq.3

$$Q_{loss} = \beta e^{\left(-\frac{E_a}{RT_{battery}}\right)}(A_h)^z \quad (3)$$

Where Q_{loss} and β denote is the capacity loss and the exponential factor respectively. As for the variable Ea, R, $T_{battery}$, A_h and z, each of them represents the activation energy, the gas constant, temperature of the battery, capacity and the power law factor. Under certain assumptions, the battery's theoretical lifespan is defined by Eq.4

$$\lambda_{min} = \int_0^{EOL} |\, I_{Bmin}(t)|dt \quad (4)$$

In this equation, the battery's life is λ_min and I_min (t) at the minimum current point. With 20% allowable loss. This formula can be used to represent the battery in Eq.5

$$\lambda_{min} = \left[\frac{20}{\beta e^{\frac{\alpha+\beta I_{Bmin}}{RT_{min}}}}\right]^{\frac{1}{z}} \quad (5)$$

The service factor, which is related to the battery's rating, is defined by Eq.6

$$\sigma = \frac{\lambda_{min}}{\lambda} \quad (6)$$

The battery is assumed to operate at 25 °C in this instance as it is well-established that the temperature control system facilitates more graceful cell aging. The battery is heated and cooled by thermal management regulates current entry and exit during driving and regenerative breaking. The nominal SOC for the battery is in Eq.7

$$SOC = \frac{\left(-V_{OC} - \sqrt{\left({V_{OC}}^2 - 4r_{battery}P_{battery}\right)}\right)}{2q_{battery}r_{battery}} \quad (7)$$

Where V_{OC} and $q_{battery}$ are open circuit voltage and the capacity of the battery. As for the DOD it is stated in

$$DOD = \int_0^t \left|\frac{P_{battery}(t)}{q_{battery}}\right| dt \quad (8)$$

Table 3. Battery parameter based on matlab battery discharge block

Battery Parameters	Values
Maximum capacity	100 Ah
Open-circuit voltage	75 V
Fully charge voltage	116.40 V
Nominal discharge current	43.48 A
Capacity at Nominal voltage	90.43 Ah

a. Parameter obtained from MATLAB battery discharge block.

Nominal discharge current is the maximum current a battery can safely discharge which significantly influenced by the SOC and DoD of battery. Understanding the nominal discharge current allows better management on battery performance.

It provides a baseline for understanding how a battery can perform under specific conditions. From Fig. 3 the battery can operate up to 6.5 hours at a single charging time.

Journal of Information Systems Engineering and Management
2025, 10(36s)
e-ISSN: 2468-4376
https://www.jisem-journal.com/

Research Article

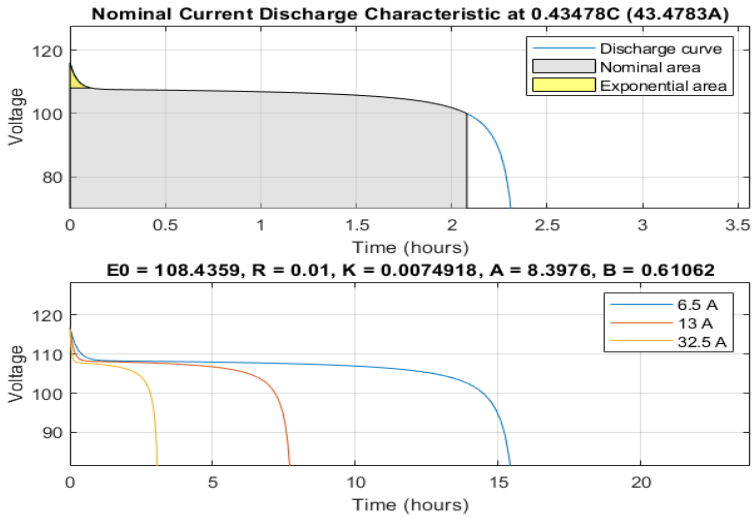

Figure. 3. Battery Nominal Current Discharge Characteristic

PMP AND ANN SOLUTION FOR ENERGY MANAGEMENT

The first step of this research is to collect the initial SOC levels and real-time speed profiles using a shooting and PMP method based on enhanced DODs or Lower SOC limits.

Battery SOC Data Collection

The first step of this research is to collect the initial SOC levels and real-time speed profiles. These speed profile data is obtained from Hongkong China of a tourist car with a 50km total of round trip. The speed profile is gathered all for the purpose of identifying the ideal lower SOC and their corresponding DoD.

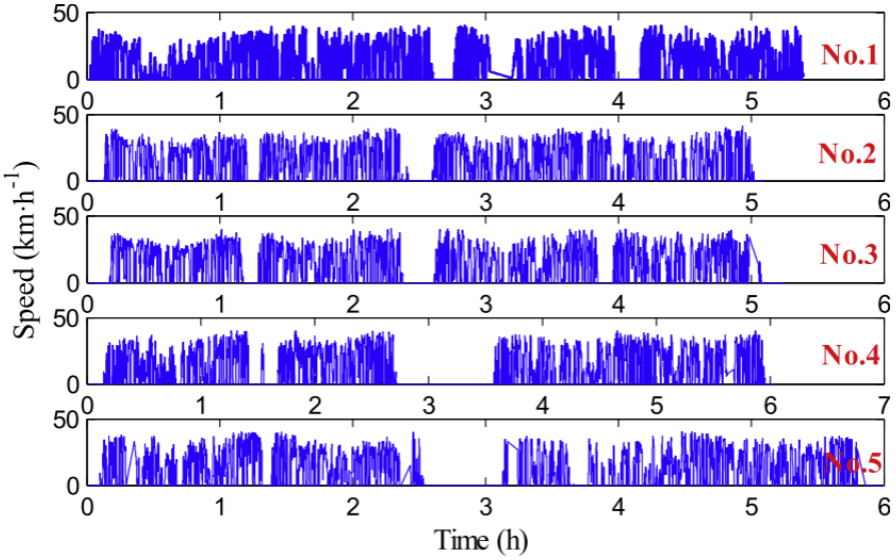

Figure 4. Speed profile of the tourist car in a round trip

Journal of Information Systems Engineering and Management
2025, 10(36s)
e-ISSN: 2468-4376
https://www.jisem-journal.com/

Research Article

Pontryagin's Minimum Principle (PMP)

Pontryagin's Minimum Principle (PMP) is one of the most effective for the purposes of optimizing battery systems [16]. In this case, the cost of energy utilization, CEU and cost of the energy battery life-cycle, CEBLC is optimized to improve energy efficiency, total operating cost and longevity of the battery system [17].

Eq.9 represents the total cost of energy utilization, $Cost_{EU}$ during the trip. This represents the combination of the fuel consumed by the energy generation unit (EGU) and the energy drawn from the battery. The equation integrates these costs over the trip duration, t_d.

$$Cost_{EU} = \int_0^{td} \left(c_f \dot{m}_f + c_e \frac{\dot{P}_{battery}}{3600} \right) dt \qquad (9)$$

The term of $C_f \dot{m}_f$ represents the cost related to fuel usage where, C_f is the unit price for fuel in CNY per liter and C_e is the unit price for electricity in CNY per kilowatt-hour. The fuel rate represents as $\dot{m}_f$ in liter per second. Dividing the energy drawn from the battery by 3600 is to convert the energy from watt-seconds to watt-hours.

Another factor that needs to be included in PMP is the total cost of battery degradation, $Cost_{EBD}$. This cost is important for the long-term impact of battery usage on its lifespan and associated replacement costs [18]. Where C_p is the cost of battery's capital in CNY per kilowatt-hour.

$$Cost_{EBD} = \int_0^{td} \left(c_p \frac{\sigma I_B}{3600 \lambda_{min}} \right) dt \qquad (10)$$

Next, the cost function is added into Eq.11 to formulate the overall optimization problem for the energy management system.

$$J = \int_0^{td} \left(c_f \dot{m}_f + c_e \frac{P_{battery}}{3600} + c_p \frac{\sigma I_B}{3600 \lambda_{min}} \right) dt \qquad (10)$$

Thus, the cost function of J and the SOC dynamic is combined together in the Hamiltonian, H of Eq.12

$$H = c_f \dot{m}_f + c_e \frac{P_{battery}}{3600} + c_p \frac{\sigma I_B}{3600 \lambda_{min}} + \lambda \dot{SOC} \qquad (11)$$

Next is to minimize the Hamiltonian which involve in finding the value of control that makes the Hamiltonian as small as possible for each point in a time. This ensures that the system operates in an optimal manner, balancing CEU and CEBLC.

$$\mathrm{P} = \arg min \, \mathrm{H} \qquad (12)$$

In this equation, the $\dot{\lambda}$ is the costate variable of SOC which is governed by the co-state dynamics Eq.14

$$\dot{\lambda} = -\frac{\partial H}{\partial SOC} = -\lambda \frac{\partial SOC_{ref}}{\partial SOC} \qquad (13)$$

The SOC is selected by equation is described in Eq.15

$$\dot{\mathrm{SOC}} = -\frac{\partial \mathrm{H}}{\partial \lambda} \qquad (14)$$

Shooting Method as PMP Solution

Since PMP does not have an analytical solution, numerical solutions are obtained by using the shooting method. The optimal DoD is determined using a variable representing the lower State of Charge SOC limit.

The first step of this research is to collect the initial SOC levels and real-time speed profiles using a shooting and PMP method based on enhanced DODs or Lower SOC limits

Journal of Information Systems Engineering and Management
2025, 10(36s)
e-ISSN: 2468-4376
https://www.jisem-journal.com/

Research Article

$$\lambda_i = \lambda_{i-1} + \varphi, \qquad i = 1,2,3,\dots n_s \tag{15}$$

Where i is the number of times taken for shooting in n_s , λ_i is the initial and φ is incremental costate value in each shooting [11].

When solving the optimal control problem by using PMP and the Shooting Method (SM) for SOC in a battery system, certain criteria must be fulfilled to achieve a valid and feasible solution.

$$\begin{gathered} SOC_{initial} = SOC_i \\ SOC_{ref} = SOC_f \\ P_{batt_{min}} \le P_{batt} \le P_{batt_{max}} \\ I_{b_{min}} \le I_b \le I_{b_{max}} \end{gathered} \tag{16}$$

The detailed flowchart of the shooting method is presented in **Error! Reference source not found.**, where n is t he shooting time and with the maximum value of 20, the parameter ε is used to control the shooting time and computational accuracy, which is specified as 0.001. Furthermore, the values of λ and φ is set to -64.5 and 0.05 respectively.

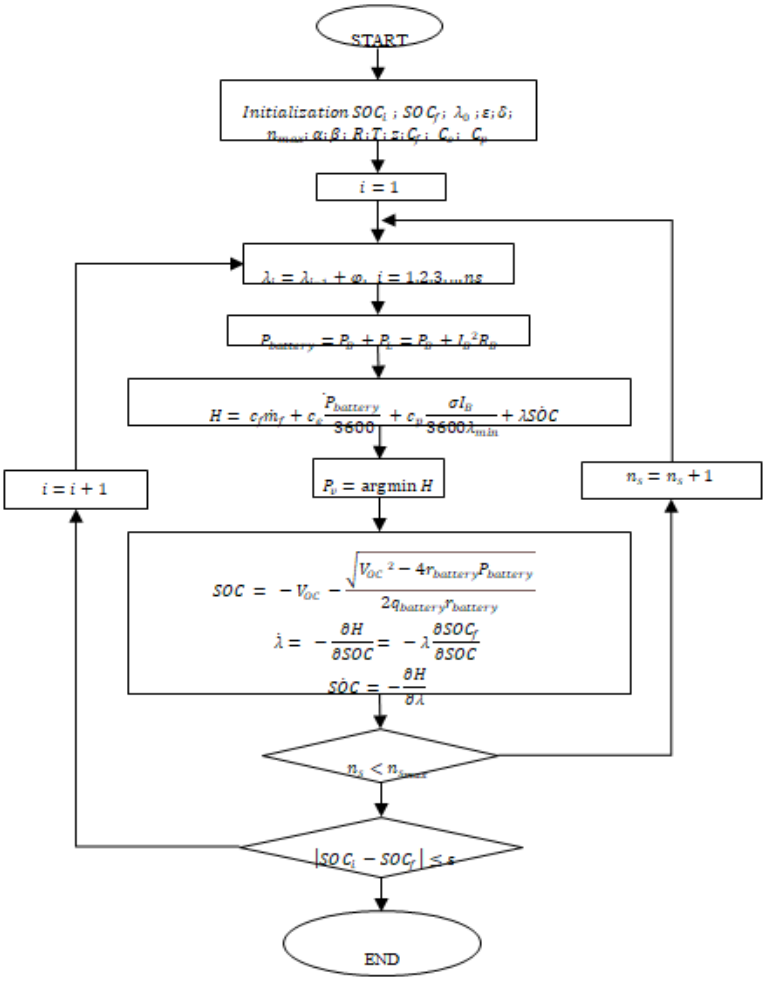

Figure 5. Flowchart of Shooting Method as Ponytryagin's Minimum Principle (PMP)

Journal of Information Systems Engineering and Management
2025, 10(36s)
e-ISSN: 2468-4376
https://www.jisem-journal.com/

Research Article

Artificial Neural Network (ANN)

Differential Function Fitting Neural Based Neural Network is an artificial neural network topology to estimate the derivative of a function [19]. The activation function of the proposed ANN is shown in Eq.18.

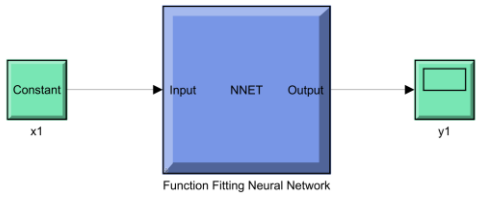

Figure. 6. Differential Function Fitting Neural Network Block Diagram

$$(i - e^{-x})^{-1} \qquad (17)$$

The ANN has three layers built for training to improve accuracy and computational power. These three neural network layers consist of an input layer, hidden layer and output layer [20].

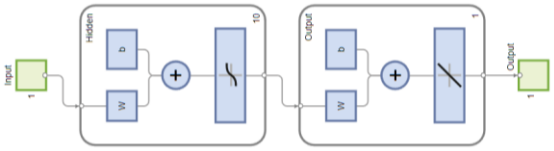

Figure. **7.** ANN Three Layer Block Diagram

The learning objective and the ANN learning ratio are set at 0.00004 and 0.1, respectively. There are eight nodes in the middle layer and the iteration time is 100. By using the first speed profile data, ANN-3 (No-1&3), and ANN-5 (No-1, 3 &5), respectively, three ANNs are structured. The data set created from the initial SOCs, and speed profiles serves as the foundation for ANN training. This proposed solution has 3 input layers which consist of power demand, battery SOC and distance travel.

SIMULATION RESULT AND DISCUSSION

The proposed PHEV battery management system was developed and simulated in MATLAB/Simulink software. Fig. 8 shows the powertrain of PHEV which is controlled by ANN. The powertrain is supplied with supercapacitor and lithium-ion battery system.

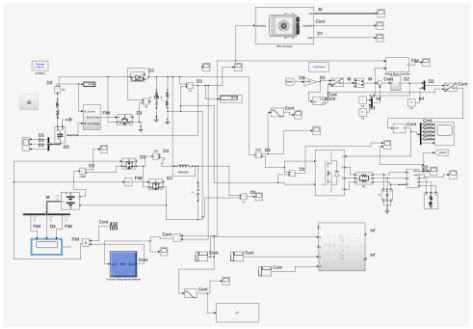

Figure. 2. PHEV Powertrain Simulation

Three ANNs are chosen by using 1, 3, and 5 layers, respectively were tested using the No. 3 speed profile. Three initial SOC 0.99, 0.96, and 0.93 were used to represent high, medium, and low starting battery charge. Dynamic Programming (DP) and Pontryagin's Minimum Principle (PMP) optimization methods were used as benchmarks for comparison with the ANNs. All simulations were performed in MATLAB R2024a on a laptop with a 3.3 GHz CPU and 24GB of RAM. Study shows that electrical energy from the battery is more expensive than fossil fuels. Therefore,

Journal of Information Systems Engineering and Management
2025, 10(36s)
e-ISSN: 2468-4376
https://www.jisem-journal.com/

Research Article

the battery is used more extensively to minimize costs until the SOC reaches a lower limit which is set to 0.2 in this case. This lower SOC is for methods without a battery aging model which allows a fair comparison with the ANNs.

For the PMP and shooting method, the final SOC, SOC_f is set at 0.3, while the initial costate μ_0 −64.5. The parameter φ is given as 0.05, and the maximum iteration count N_{max} is set to 20. Additional constants such as α, β is −15700 and 170.3 respectively. As for the cost of C_f, C_e, C_p is assigned to a value of 1.1, 3.2 and 3200 respectively. The parameters Z, T, and R are specified as 0.48, 297.15, and 8.31 respectively. These values form the basis for the simulation model, ensuring accurate and consistent calculations

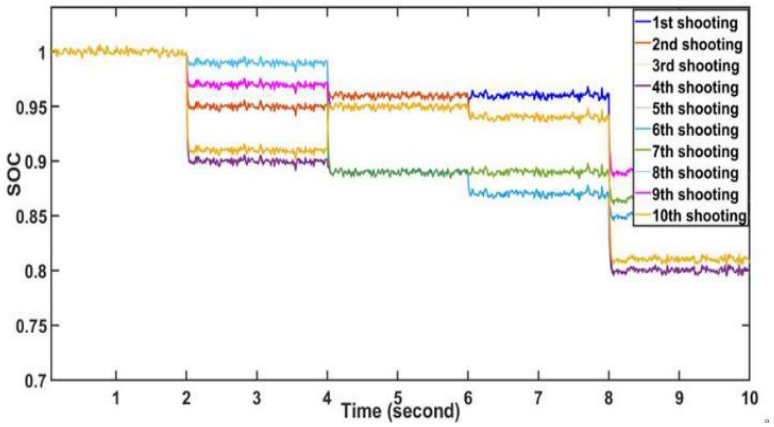

(a)

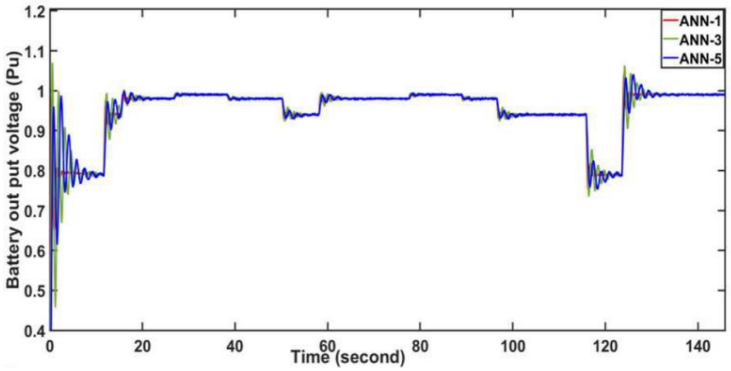

(b)

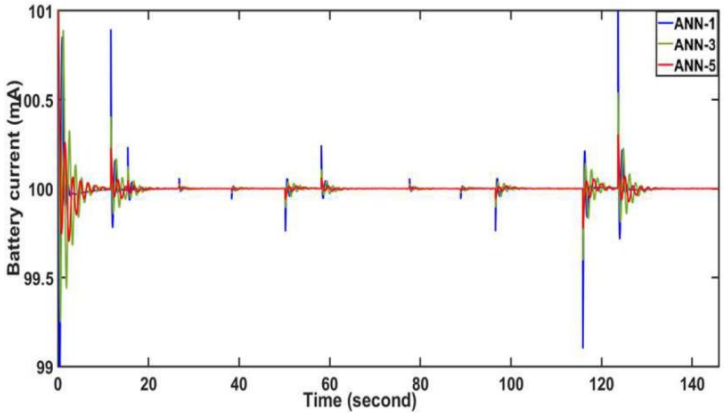

(c)

Journal of Information Systems Engineering and Management
2025, 10(36s)
e-ISSN: 2468-4376
https://www.jisem-journal.com/

Research Article

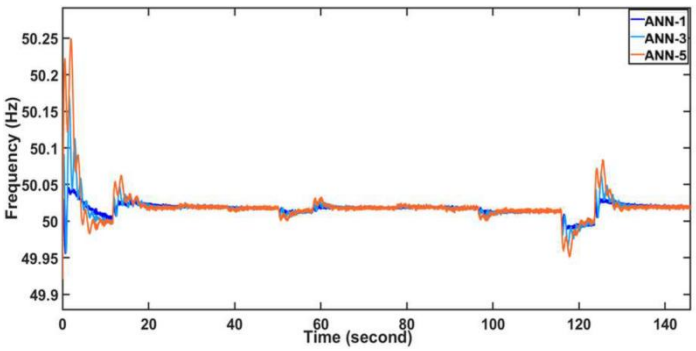

(d)

Figure 9. Battery Performance during the trip (simulation) (a) Battery State of Charge (b) Battery Voltage (c) Battery Current (d) System Frequency

The SOC profile graph illustrates the battery's state of charge changes over time during the energy management process. The number of shooting track different optimization phases as SOC gradually declines until it reaches the optimal depth of discharge (DOD). This controlled decrease shows a successful energy distribution between battery and engine systems thus maximizing the use of stored energy. The stabilization of SOC toward the end highlights the system's ability to balance energy demands dynamically. The EMS demonstrated stable operation across multiple iterations reflects a successful maintaining SOC within acceptable limits of SOC levels by using ANN and PMP strategies. This balance helps preserve battery life and optimize fuel consumption throughout the driving cycle.

The battery output voltage graph demonstrates the voltage variations during the trip for ANN-1, ANN-3, and ANN-5 models. The ANN models exhibit sustained alignment in voltage profiles despite load condition changes which show the system is reliable and consistent. The stabilization of voltage after disturbances indicates that the EMS efficiently handles load balancing which can avoid significant voltage spikes or drops. This stability contributes to improved system reliability and prevents strain on the battery, which is essential for extending battery life. The similarities between ANN models indicate that ANN-based Energy Management Systems (EMS) are reliable and perform consistently in various situations. This reliability is further enhanced by the ability to regulate voltage, which improves the overall energy efficiency of plug-in hybrid electric vehicles (PHEVs).

From approximately 20 seconds to the end of the simulation, the battery current for all three ANN methods remains stable around 100 mA, with only minor fluctuations. This indicates that the control strategies implemented by ANN-1, ANN-2, and ANN-3 are effective at maintaining consistent current during steady-state operation. From the graph, the current is seen to have a significant spike in battery current around 0-20 seconds and around 120 seconds. These spikes indicate the system is responding to changes in load or operating conditions. ANN-1 appears to exhibit slightly higher transient spikes compared to ANN-2 and ANN-3, indicating that it may be less optimized for transient stability. Despite minor differences, the overall alignment of the methods suggests comparable performance. The steady current range of 99-101 mA indicates effective control and efficient energy utilization. This consistent current level is crucial for maintaining battery health and extending its lifespan.

As for the system frequency graph, this graph highlights the frequency variations observed during the trip for ANN-1, ANN-3, and ANN-5 models. It can be seen that profiles are nearly identical to each other. This indicates the stability performance of the EMS proves effective through these consistent profiles which maintain grid or system frequency stability. The consistent behavior reflects the adaptability of the ANN-based EMS in adapting to dynamic conditions without compromising system performance. The stability of frequencies across hybrid systems plays a critical role in scenarios where load changes occur frequently. This graph further confirms the ANN models are effective in supporting real-time energy management while preserving system stability.

In Fig. 3, the graphs illustrate SOC profiles for three different ANN models (ANN-1, ANN-3, and ANN-5) under a specific speed profile. All ANN models demonstrate dynamic control over the battery's SOC, exhibiting consistent behavior. Notably, ANN-5 exhibits superior stability during the initial fluctuations results from a wider training algorithm datasheet.

Journal of Information Systems Engineering and Management
2025, 10(36s)
e-ISSN: 2468-4376
https://www.jisem-journal.com/

Research Article

Fig. 3 (b) and (c) compare ANN-based methods with PMP, where ANN models exhibit superior performance in maintaining a controlled SOC profile. PMP shows steeper declines in SOC, reflecting less precise energy utilization. ANN-3 and ANN-5 are seen to maintain SOC closer to the optimal range which indicates better adaptability to real-time conditions. ANN-based methods surpass better in balancing battery usage with energy efficiency thus reducing unnecessary energy consumption while ensuring stability. This highlights the ANN's ability to learn complex patterns from training data. ANN-based had outperformed rule-based methods like PMP in both preserving battery life and enhancing system reliability during the trip.

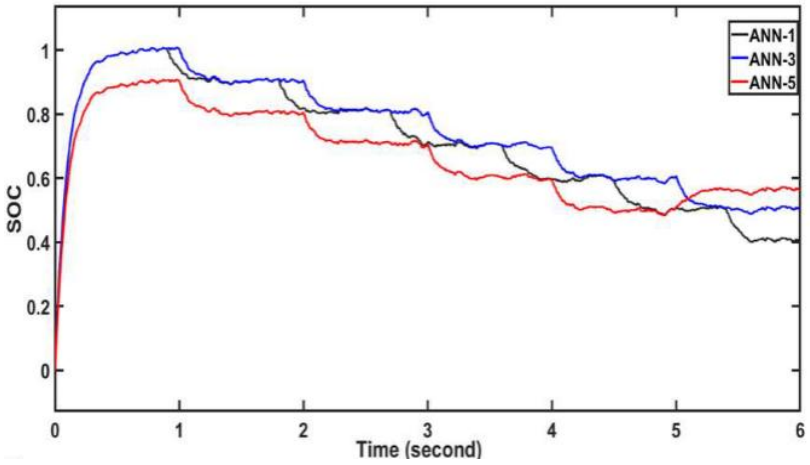

(a)

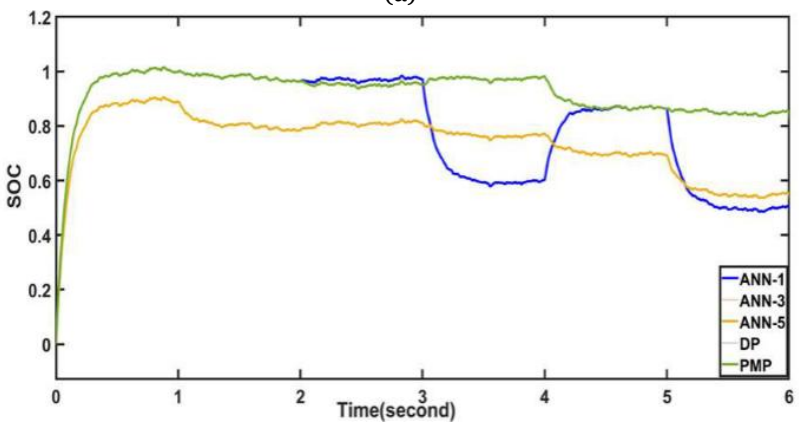

(b)

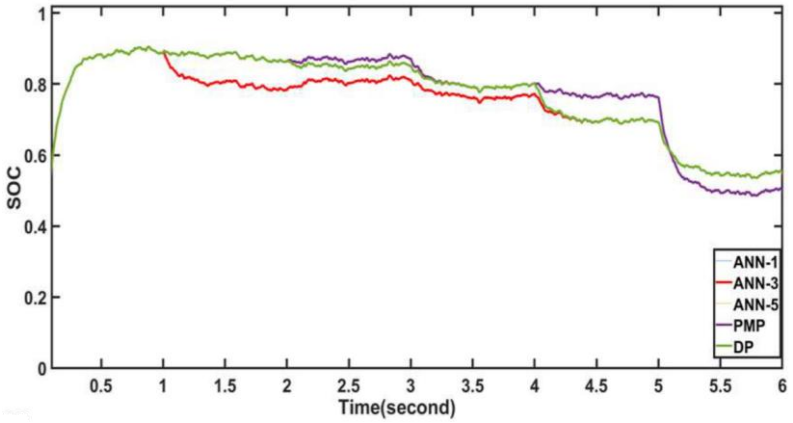

(c)

Fig. 3 State of Charge Profile created using speed profile number 3 by using 5 types of method (a) Initial SOC 0.99 (b) Initial SOC 0.96 (c) Initial SOC 0.93

Journal of Information Systems Engineering and Management
2025, 10(36s)
e-ISSN: 2468-4376
https://www.jisem-journal.com/

Research Article

Fig. 3 show the SOC profiles for different strategies and initial SOCs. Both PMP and DP reach the specified lower SOC boundary of 0.2 when a lower limit is enforced. The SOC profiles generated by the three ANNs closely resemble those of PMP with the same initial SOC. However, there are differences in how quickly the SOC changes. PMP and DP show more sudden changes in SOC compared to the ANN models.

Table IV. Summarizes the comparative performance of ANN-based methods of ANN-1, ANN-3, and ANN-5 in terms of fuel cost, energy utilization, Cost of Energy Battery Degradation ($Cost_{EBD}$) and total cost. In some cases, PMP and DP method performs specific strengths in certain area. However, overall, ANN-based method outperforms them in a balanced and practical manner.

ANN-1 and ANN-5 achieve competitive fuel costs across different SOC initial conditions. For example, at SOCi = 0.99, ANN-1 uses only 7.91 L, slightly lower than PMP's 8.10 L, [why]. Other than that, ANN methods provide optimized energy use, with ANN-1 and ANN-3 showing values within a narrow, efficient range compared to PMP's higher utilization at SOCi = 0.99 (17.69 kWh). This balance makes ANN methods suitable for systems requiring consistent energy conservation. Lastly, the total cost of ANN-1 is consistently among the lowest across all SOC levels. At SOCi = 0.96, ANN-1 achieves a total cost of 59.16 CNY, significantly better than DP's 69.06 CNY, making it a cost-effective solution for practical applications.

The performance evaluation of ANN-based methods indicates successful energy management which accomplishes

better performance than PMP and DP in multiple criteria. The effective optimization of fuel consumption and energy distribution results in reduced total costs through ANN-1 and ANN-3 methods. ANN models achieve better fuel efficiency than PMP techniques while using less energy than DP procedures thereby finding the optimal ratio between operational cost factors. ANN-3 performs consistently well by lowering fuel usage while keeping energy usage moderate and achieving lower total costs across all SOC range operations. ANN proves superior due to its excellent ability to detect complex nonlinear patterns between data points and dynamically adapt to operational changes which delivers optimized results with lower computational requirements than DP methods. Since ANN methods benefit from both scalability and real-time determination abilities, they demonstrate suitable applications for energy management systems that balance their operational expense with performance output effectively.

TABLE 4. Comparison of Equivalent Computational Cost with Other Method

Method	SOC_i	*Fuel Cost (L)*	*Energy Utilize (kWh)*	$Cost_{EBD}$ *(CNY)*	*Total Cost (CNY)*
PMP		*8.10*	*17.69*	*10.85*	*58.98*
DP		*1.78*	*28.42*	*13.09*	*61.28*
ANN1	*0.99*	*7.91*	*16.44*	*11.78*	*58.08*
ANN3		*8.22*	*16.36*	*11.77*	*59.08*
ANN5		*8.22*	*16.40*	*11.78*	*59.11*
PMP		*8.11*	*16.67*	*11.91*	*69.06*
DP		*2.99*	*22.73*	*14.91*	*70.41*
ANN1	*0.96*	*8.29*	*14.16*	*10.78*	*59.16*
ANN3		*7.31*	*17.14*	*10.77*	*59.17*
ANN5		*7.31*	*14.12*	*10.77*	*59.19*
PMP		*8.39*	*14.76*	*11.79*	*59.51*
DP	*0.93*	*5.85*	*19.41*	*10.31*	*59.52*
ANN1		*7.46*	*13.61*	*11.77*	*59.32*

Journal of Information Systems Engineering and Management
2025, 10(36s)
e-ISSN: 2468-4376
https://www.jisem-journal.com/

Research Article

ANN3	*7.53*	*13.37*	*9.71*	*59.31*
ANN5	*7.51*	*13.45*	*9.73*	*59.35*

CONCLUSION

This study presents a data-driven differential function fitting neural based neural network energy management system (DEMS) for Plug-in Hybrid Electric Vehicles (PHEVs) using an Artificial Neural Network (ANN) and Pontryagin's Minimum Principle (PMP) to enhance both energy efficiency and battery usage. The proposed system utilizes a modified three-layer backpropagation ANN the real time speed profile incorporated into the system allowing dynamic energy management that changes to meet different conditions of driving and initial state-of-charge (SOC). Using real time speeds can determines the optimal usage of energy between the battery and the gasoline engines to minimize fuel and energy wastage. The choice of an optimal depth of discharge (DOD) preserves the battery function lying within the best level and contributing to the battery's durability. This approach shows that energy consumption costs are reduced by 15.99%; 15.97% and 23.13% for SOC levels of 0.99, 0.97 and 0.95 respectively with enhancements in fuel consumption and battery life. Moreover, the system shows almost identical behavior throughout various driving situations indicating versatility and stability of the system. By virtue of the structure of the ANN the system can be implemented as a real time system in PHEVs, making energy management possible in real life. The present study describes how energy management systems developed through neural networking can revolutionize vehicle performance, decrease expenditure and optimize battery performance. Further investigation of the selected methods will be devoted to enlarging the parameter set and fine-tuning of the model to enhance the system's ability to respond to real-world driving conditions.

ACKNOWLEDGMENT

This research is funded by Universiti Teknologi MARA under the Special Research Grant [Geran Penyelidikan Khas 600-RMC/GPK 5/3 (129/2020)]. Authors would also like to acknowledge College of Engineering, UiTM for the excellent facility provided to carry out this research

REFERENCES

[1] Z. Chen, R. Xiong, and J. Cao, "Particle swarm optimization-based optimal power management of plug-in hybrid electric vehicles considering uncertain driving conditions," Energy, vol. 96, pp. 197–208, Feb. 2016, doi: 10.1016/j.energy.2015.12.071.

[2] H. Singh, A. Ambikapathy, K. Logavani, G. Arun Prasad, and S. Thangavel, "Plug-In Hybrid Electric Vehicles (PHEVs)," 2021, pp. 53–72. doi: 10.1007/978-981-15-9251-5_3.

[3] H. Cai et al., "Degradation Evaluation of Lithium-Ion Batteries in Plug-In Hybrid Electric Vehicles: An Empirical Calibration," Batteries, vol. 9, no. 6, p. 321, Jun. 2023, doi: 10.3390/batteries9060321.

[4] B. Xu, A. Oudalov, A. Ulbig, G. Andersson, and D. S. Kirschen, "Modeling of Lithium-Ion Battery Degradation for Cell Life Assessment," IEEE Trans Smart Grid, vol. 9, no. 2, pp. 1131–1140, Mar. 2018, doi: 10.1109/TSG.2016.2578950.

[5] B. Sakhdari and N. L. Azad, "An Optimal Energy Management System for Battery Electric Vehicles," IFAC-PapersOnLine, vol. 48, no. 15, pp. 86–92, 2015, doi: 10.1016/j.ifacol.2015.10.013.

[6] P. Li, Y. Li, Y. Wang, and X. Jiao, "An Intelligent Logic Rule-Based Energy Management Strategy for Power- Split Plug-in Hybrid Electric Vehicle," in 2018 37th Chinese Control Conference (CCC), IEEE, Jul. 2018, pp. 7668–7672. doi: 10.23919/ChiCC.2018.8483062.

[7] A. Graa and F. Benhamida, "A review on optimization methods applied to energy management system," Serbian Journal of Management, vol. 15, no. 2, pp. 371–382, 2020, doi: 10.5937/sjm15-22519.

[8] Z. Chen, R. Xiong, B. Liu, Z. Wang, and Q. Yu, "Pontryagin's Minimum Principle-Based Power Management of Plug-In Hybrid Electric Vehicles to Enhance the Battery Durability and Thermal Safety," IEEE Transactions on Transportation Electrification, vol. 9, no. 4, pp. 5039–5048, Dec. 2023, doi: 10.1109/TTE.2022.3201029.

[9] M. S. Alam and S. A. Arefifar, "Energy Management in Power Distribution Systems: Review, Classification,

Research Article

Limitations and Challenges," IEEE Access, vol. 7, pp. 92979–93001, 2019, doi: 10.1109/ACCESS.2019.2927303.

[10] T. Etem, "Machine Learning Approaches for Predicting Electric Vehicle Charging Demand and Energy Consumption," in 2024 8th International Artificial Intelligence and Data Processing Symposium (IDAP), IEEE, Sep. 2024, pp. 1–7. doi: 10.1109/IDAP64064.2024.10710701.

[11] S. Xie, X. Hu, S. Qi, and K. Lang, "An artificial neural network-enhanced energy management strategy for plug-in hybrid electric vehicles," Energy, vol. 163, pp. 837–848, Nov. 2018, doi: 10.1016/j.energy.2018.08.139.

[12] S. Jain and L. Kumar, "Fundamentals of Power Electronics Controlled Electric Propulsion," in Power Electronics Handbook, Elsevier, 2018, pp. 1023–1065. doi: 10.1016/B978-0-12-811407-0.00035-0.

[13] X. Lin, K. Zhou, and H. Li, "AER adaptive control strategy via energy prediction for PHEV," IET Intelligent Transport Systems, vol. 13, no. 12, pp. 1822–1831, Dec. 2019, doi: 10.1049/iet-its.2018.5582.

[14] T. Wang et al., "Capacity degradation analysis and knee point prediction for lithium-ion batteries," Green Energy and Intelligent Transportation, vol. 3, no. 5, p. 100171, Oct. 2024, doi: 10.1016/j.geits.2024.100171.

[15] M. RASHID, "Li-ion batteries life cycle from electric vehicles to energy storage," Aug. 2024, pp. 223–229. doi: 10.21741/9781644903216-29.

[16] N. Kim, S. Cha, and H. Peng, "Optimal control of hybrid electric vehicles based on Pontryagin's minimum principle," IEEE Transactions on Control Systems Technology, vol. 19, no. 5, pp. 1279–1287, Sep. 2011, doi: 10.1109/TCST.2010.2061232.

[17] M. Fanoro, M. Božanić, and S. Sinha, "A Review of the Impact of Battery Degradation on Energy Management Systems with a Special Emphasis on Electric Vehicles," Energies (Basel), vol. 15, no. 16, p. 5889, Aug. 2022, doi: 10.3390/en15165889.

[18] P. Gasper, N. Laws, B. Rathod, D. Olis, K. Smith, and F. Thakkar, "Optimization of Energy Storage System Economics and Controls by Incorporating Battery Degradation Costs in REopt," ECS Meeting Abstracts, vol. MA2023-01, no. 3, pp. 764–764, Aug. 2023, doi: 10.1149/MA2023-013764mtgabs.

[19] S. Ledesma, D.-L. Almanza-Ojeda, M.-A. Ibarra-Manzano, E. C. Yepez, J. G. Avina-Cervantes, and P. Fallavollita, "Differential Neural Networks (DNN)," IEEE Access, vol. 8, pp. 156530–156538, 2020, doi: 10.1109/ACCESS.2020.3019307.

[20] H. Araki and S. Omatu, "Artificial olfactory sense and recognition system," in Biomimetic Technologies, Elsevier, 2015, pp. 121–139. doi: 10.1016/B978-0-08-100249-0.00006-9.